# EXPERIMENTAL AND NUMERICAL CHARACTERIZATION OF THE ACTIVE BEHAVIOUR OF MOUSE ROTATOR CUFF MUSCLES

**P. Martins[1,2], A. Pérez[3,4], G. Abizanda[3,4], B. Calvo[1,5], J. Grasa[1,5]**

*1 Aragón Institute of Engineering Research (i3A), University of Zaragoza, Spain*
*2 Fundación Aragonesa para la investigación y desarrollo (ARAID)*
*3 Regenerative Medicine Program, Foundation for Applied Medical Research (FIMA), University of Navarra (UNAV)*
*4 Instituto de Investigación Sanitaria de Navarra (IdiSNA)*
*5 Bioengineering, Biomaterials and Nanomedicine Networking Biomedical Research Centre (CIBER-BBN), Zaragoza, Spain*

ESB2022
27th Congress of the European Society of Biomechanics
26 - 29 June 2022, Porto, Portugal

## INTRODUCTION

- **Muscle fatty infiltration after tendon rupture is responsible for muscle atrophy, and consequently, muscle function loss.**
- **This problem is more usually in rotator cuff injuries [1]. The rotator cuff is the group of muscles and tendons that act to stabilize the shoulder and allow for its extensive range of motion.**
- **The passive and active behaviour of the Infraspinatus and Supraspinatus muscles of a mice model has been analyzed.**

**Objective:** **This work establishes a new framework based on an animal model and computational simulation to understand the biomechanics of the joint and to test new treatments**

## METHODS

### Experimental characterization

The experimental study was conducted in accordance with the provisions of the European and Spanish legal normatives (RD53/2013). Isolated supraspinatus (n=3) and infraspinatus (n=3) mouse (wild-type (WT, C57BL/6J)) muscles were prepared to measure their maximum active isometric force and tested afterwards uniaxially till fracture.

### Mathematical formulation

The active and passive behavior of the muscle tissue is modelled within the continuum mechanics framework. The tissue is considered as an hyperelastic transversely isotropic material. The strain energy function is decoupled into a volume-changing and a volume-preserving parts in order to handle the quasi-incompressibility constraint:

$$\Psi = \Psi_{vol} + \underbrace{\bar{\Psi}_p\left(\bar{\boldsymbol{C}}, \boldsymbol{N}\right)}_{\text{B. Calvo et al. 2010 [2]}} + \underbrace{\bar{\Psi}_a(\bar{\boldsymbol{C}}_e, \bar{\lambda}_a, \boldsymbol{M})}_{\text{B. Hernández-Gascón et al. 2013 [3]}}$$

**Passive Behaviour**

$$\bar{\Psi}_p = c_1\left(\bar{I}_1 - 3\right) + \bar{\Psi}_{pf}$$

$$\bar{\Psi}_{pf} = \begin{cases} 0 & \bar{I}_4 < \bar{I}_{40} \\ \frac{c_3}{c_4}\left(\exp^{c_4(\bar{I}_4 - \bar{I}_{40})} - c_4\left(\bar{I}_4 - \bar{I}_{40}\right) - 1\right) & \bar{I}_4 > \bar{I}_{40} \text{ and } \bar{I}_4 < \bar{I}_{4_{ref}} \\ c_5\sqrt{\bar{I}_4} + \frac{1}{2}c_6 \ln\left(\bar{I}_4\right) + c_7 & \bar{I}_4 > \bar{I}_{4_{ref}} \end{cases}$$

**Active Behaviour**

$$\bar{\Psi}_a = f_1\left(\bar{\lambda}_a\right) f_2\left(f_r, t\right) \bar{\Psi}'_a\left(\bar{J}_4\right)$$

$$\bar{\Psi}'_a = \frac{1}{2}P_0\left(\bar{J}_4 - 1\right)^2 \qquad \bar{J}_4 = \boldsymbol{m}_0 \cdot \bar{\boldsymbol{C}}_e \boldsymbol{m}_0 = \bar{\lambda}_e$$

$$\mathbf{P}_a - \frac{\partial \bar{\Psi}}{\partial \bar{\lambda}_a} + \left(2\bar{\mathbf{C}}_e \frac{\partial \bar{\Psi}}{\partial \bar{\mathbf{C}}_e} \bar{\mathbf{F}}_a^{-T}\right) : \frac{\partial \bar{\mathbf{F}}_a}{\partial \bar{\lambda}_a} = C\dot{\bar{\lambda}}_a$$

$$C = \frac{1}{v_0}P_0 f_1(\bar{\lambda}_a) f_2(f_r, t) \quad P_a = -\nu P_0 f_1(\bar{\lambda}_a) f_2(f_r, t)$$

### Computational model

The geometry of bone and muscles was obtained from MRI image segmentation.

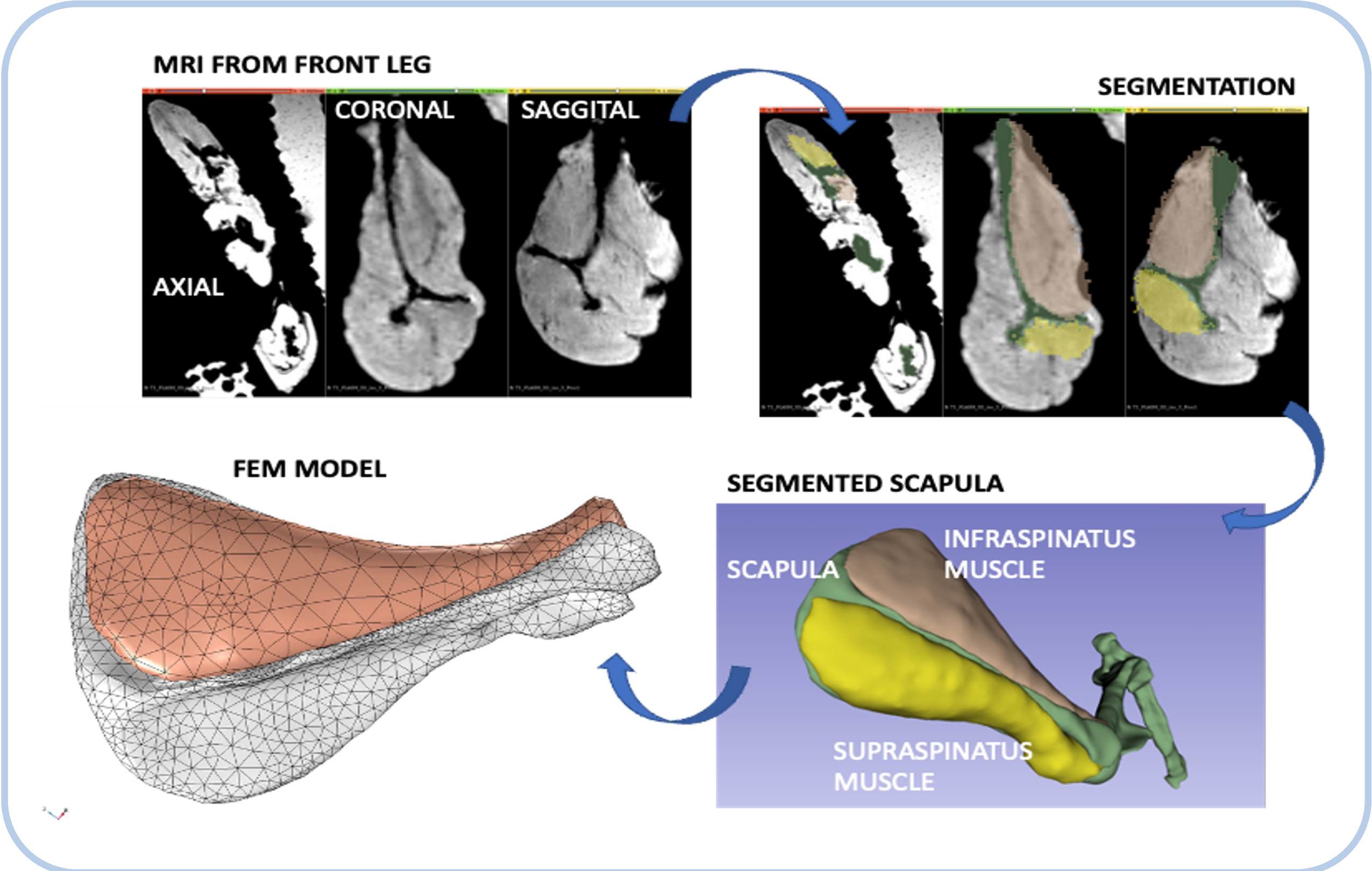

To handle the anisotropy of the material, the **muscle fibers** directions have to be incorporated into the model. These orientations were obtained using the software Comsol Multiphysics v. 5.3.

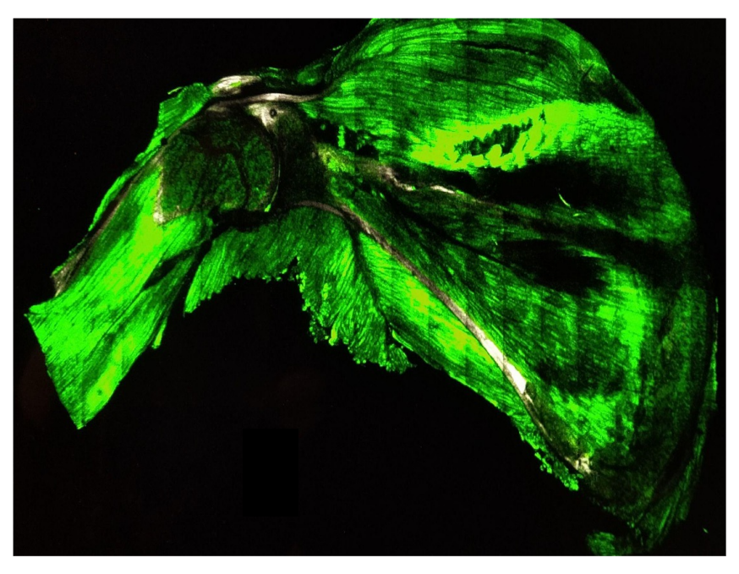

Fiber orientation was obtained by analyzing two photon confocal microscope images.

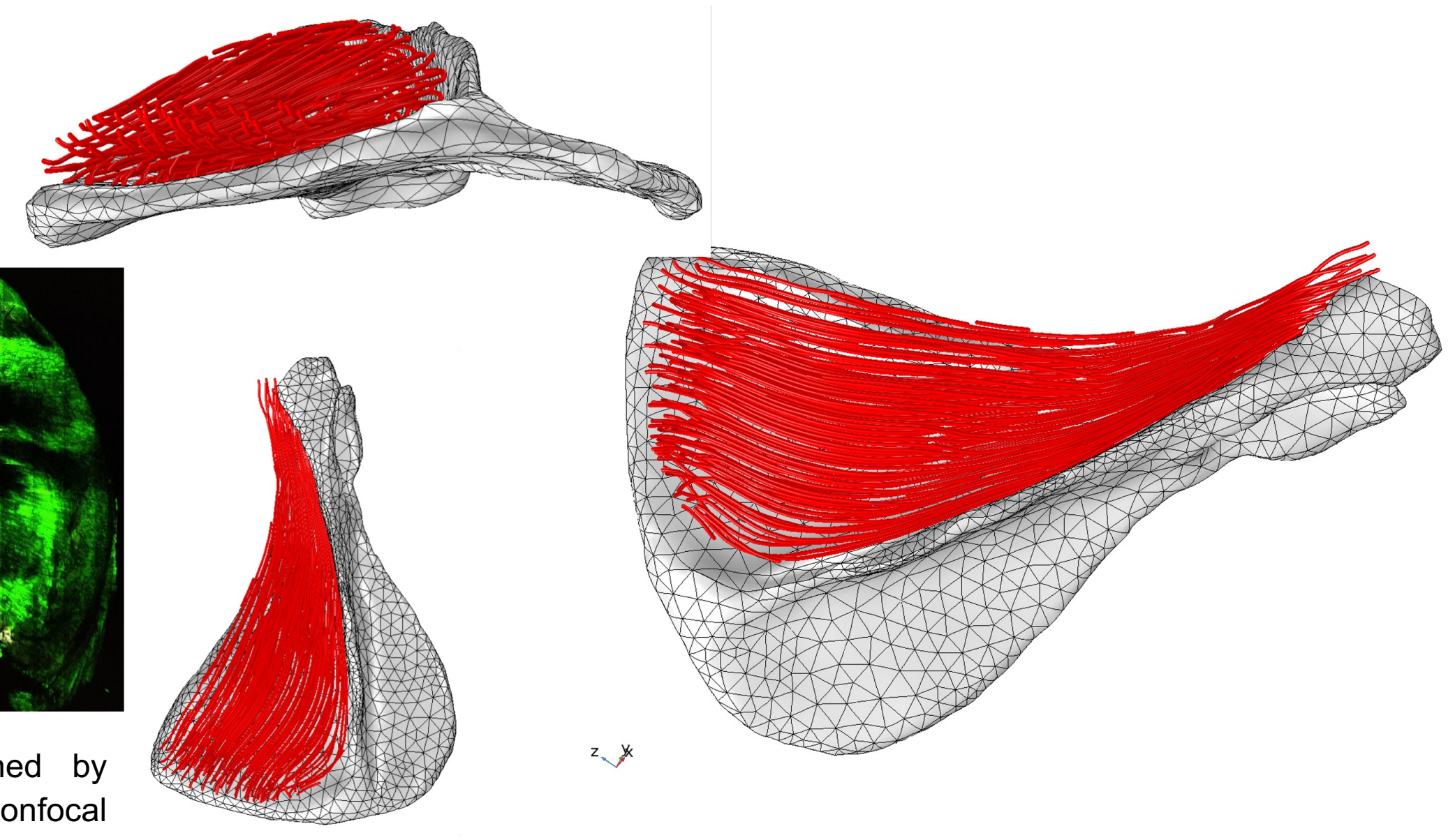

## RESULTS

Experimental force versus stretch relationships for both Infraspinatus and Supraspinatus muscles were analyzed to characterize the passive behaviour of the tissue. The parameters of the model fitting were obtained using the Levenberg-Marquardt optimization algorithm.

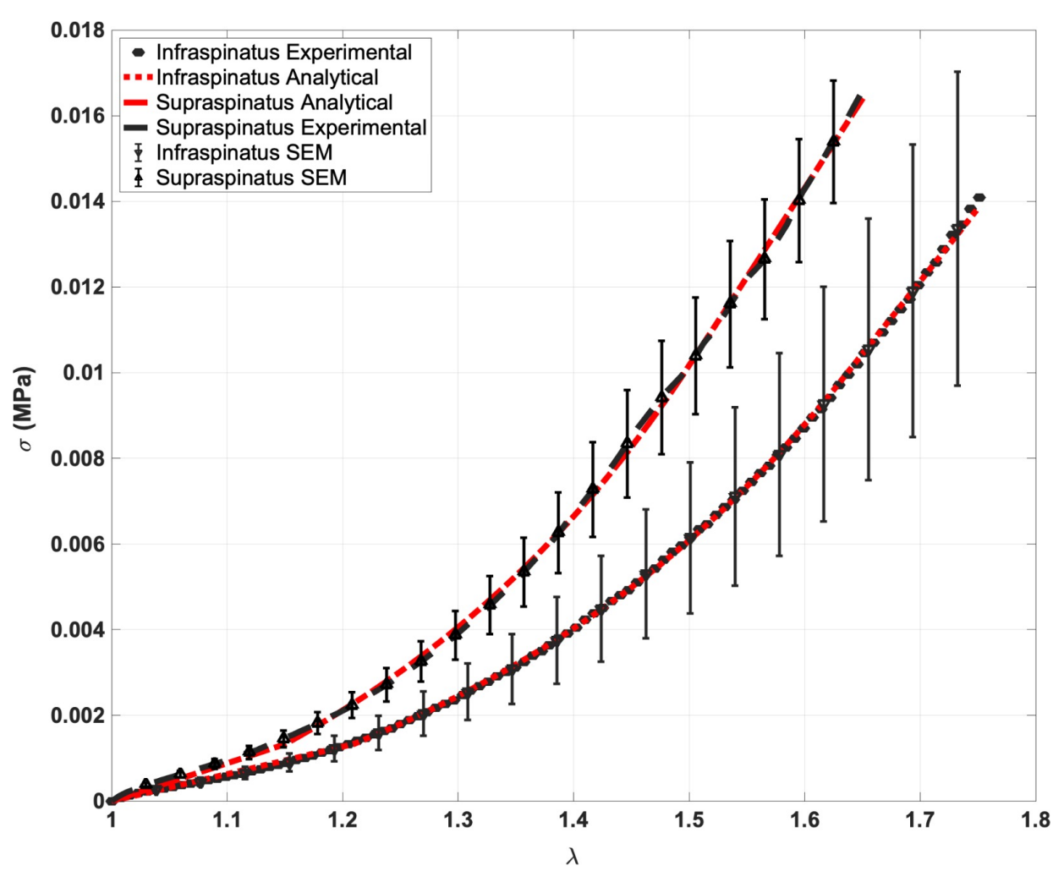

Experimental uniaxial passive tests of both muscles and numerical fitting

| Passive response parameters | | |
|---|---|---|
| | **Infraspinatus** | **Supraspinatus** |
| $c_1$ (MPa) | 0.001047 | 0.001465 |
| $c_3$ (MPa) | 0.001440 | 0.001533 |
| $c_4$ | 0.453006 | 0.634963 |
| $c_5$ (MPa) | 0.026128 | 0.031050 |
| $c_6$ (MPa) | -0.037105 | -0.04104 |
| $c_7$ | -0.023900 | -0.02941 |
| $\bar{I}_{40}$ | 1.464100 | 1.322500 |
| $\bar{I}_{4_{ref}}$ | 2.656900 | 2.250000 |

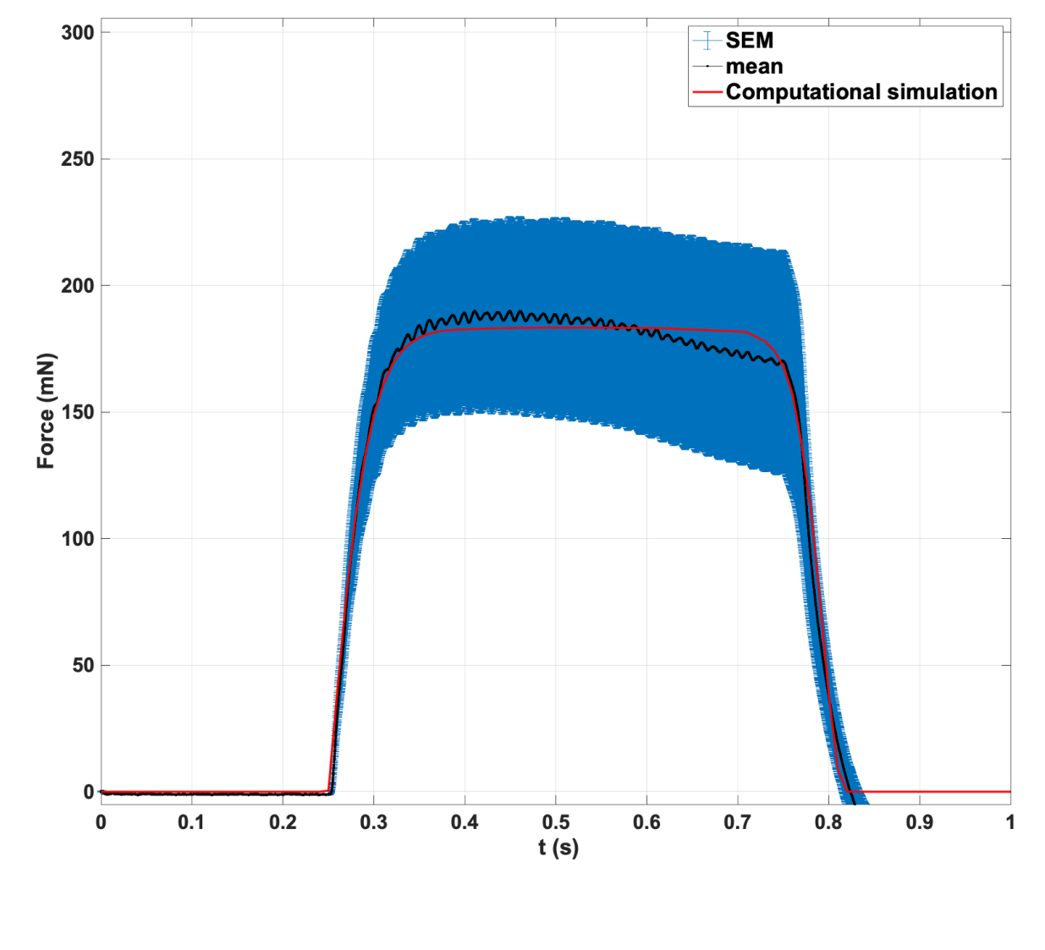

Evolution of **muscle force** (mN) during the contraction together with the computational outcome

The active response of the Infraspinatus muscle was characterized under isometric contractions of 0.5 s. The tissue was stimulated with electrical pulses of 10 ms and 100 V at 100 Hz.

| Active response parameters | |
|---|---|
| $P_0$ (MPa) | 0.4 |
| $v_0$ | 6 |
| $\nu$ | 0.59 |

### Computational Results

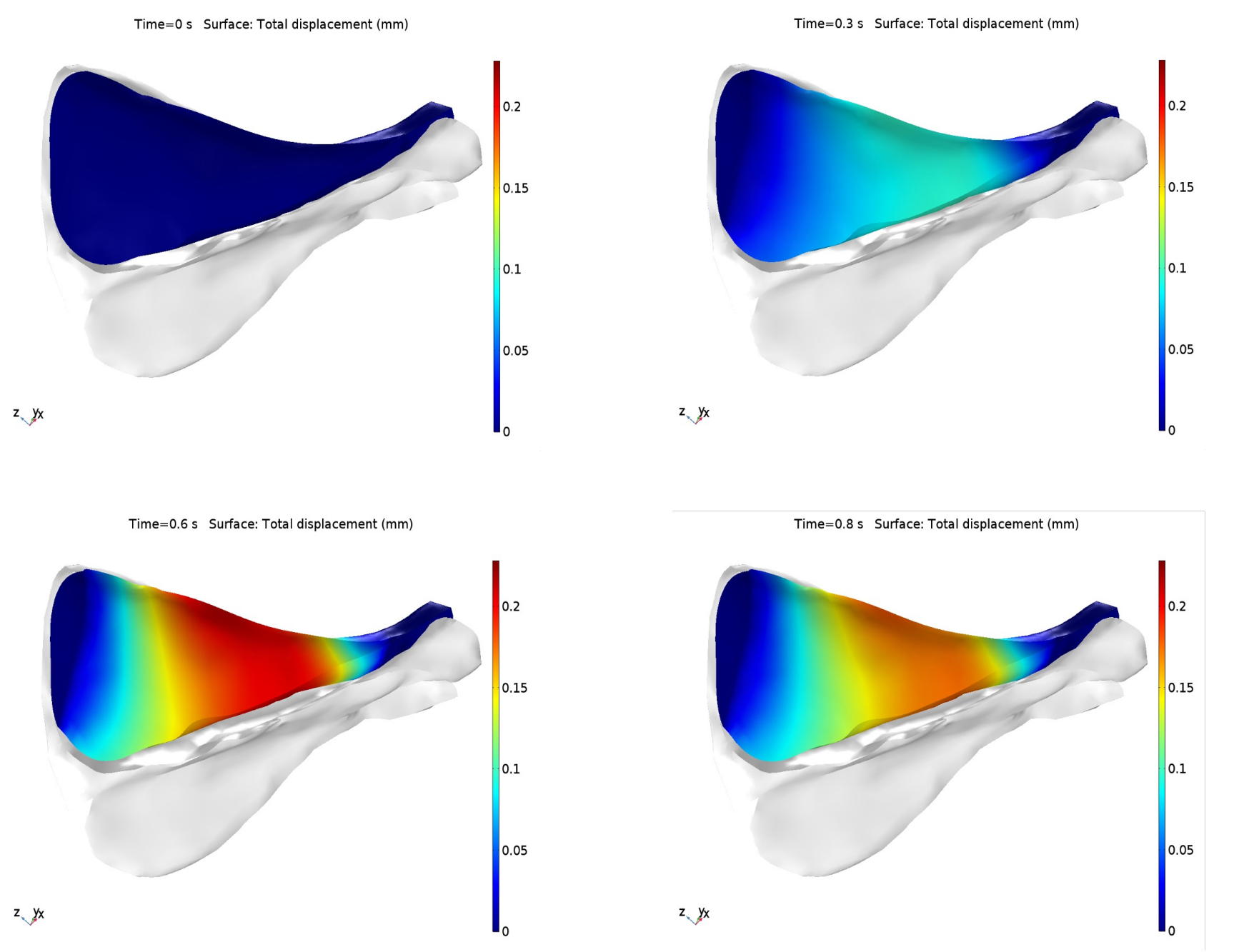

**Total displacement field (mm)** obtained during the contraction of the muscle

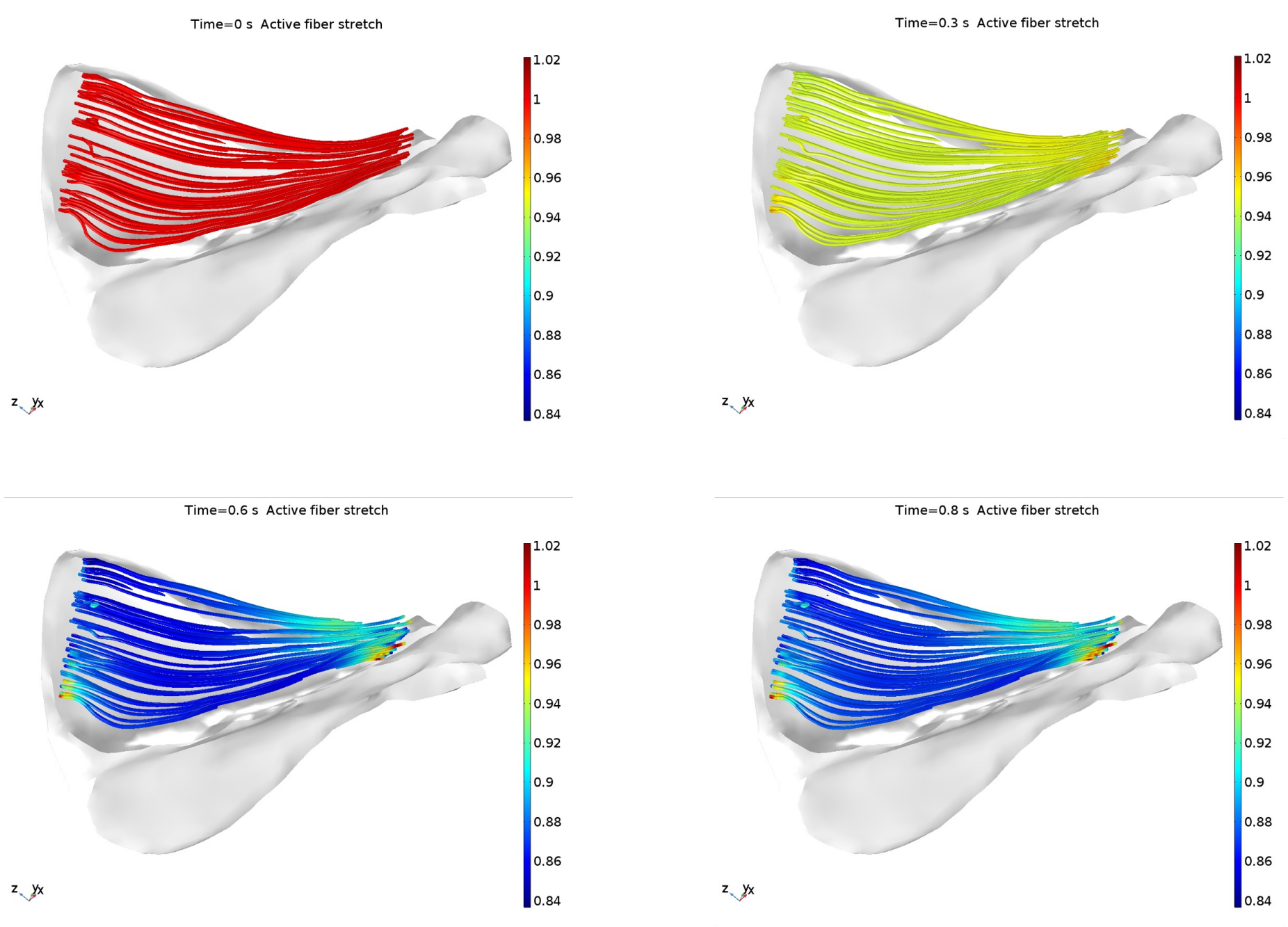

**Active fiber stretch** represented along the fiber directions used by the model discretization

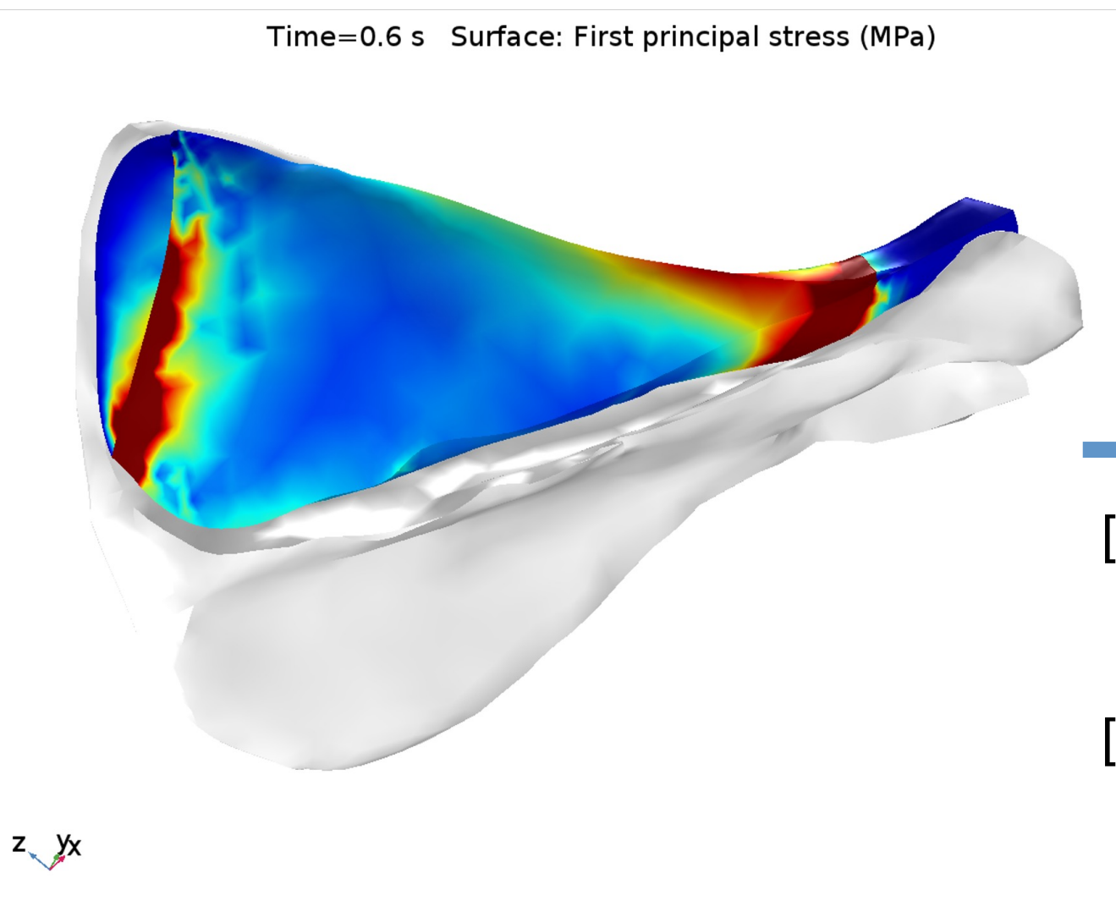

**First principal stress** (MPa) distribution along the tissue at the contraction peak.

## CONCLUSIONS

**The results show the difference in the mechanical properties of both infra and supraspinatus muscles.**

**The passive behavior shows a stiffer supraspinatus compared with the infraspinatus.**

**The maximum force of both muscles and the contractile properties according to time has also been determined. The data and fittings h-ave been used to develop the FEM simulations of the rotator cuff muscles and will be used to investigate the biomechanics and damage effects.**

## REFERENCES

[1] Shirasawa, H., Matsumura, N., Shimoda, M. et al. Inhibition of PDGFR signaling prevents muscular fatty infiltration after rotator cuff tear in mice. Sci Rep 7, 41552 (2017).

[2] Calvo B, Ramírez A, Alonso A, Grasa J, Soteras F, Osta R, Muñoz MJ. Passive nonlinear elastic behaviour of skeletal muscle: experimental results and model formulation. J Biomech. 43(2):318-25 (2010).

[3] Hernández-Gascón, B., Grasa, J., Calvo, B., Rodríguez, J. F. A 3D electro-mechanical continuum model for simulating skeletal muscle contraction. J. Theor. Biol. 335, 108–118 (2013).

## ACKNOWLEDGEMENTS

**Projects PID2020-113822RB-C21 and PID2020-113822RB-C22 funded by MCIN/AEI /10.13039/501100011033**